[34] Venkataramana, J., Degaleesan, T.E., Laddha, G.S., *Can. J. Chem. Eng 58* (1980) pp. 206–211.
[35] Zhu, S., Zhang, B., Shen, Z., Wang, J., *Chem. Ind. Eng (China)* (1982) No. 1, p. 1.
[36] Kamath, M.S., Subba Rau, M.G., *Can. J. Chem. Eng 63* (1985) pp. 578–584.
[37] Coulaloglou, C.A., Tavlarides, L.L., *Chem. Eng Sci. 32* (1977) pp. 1289–1297.
[38] Eid, K., *Thesis,* L'Institut National Polytechnique de Toulouse, France, 1984.
[39] Kumar, A., Hartland, S., *Trans. Inst. Chem. Eng 60* (1982) pp. 35–39.
[40] Mugele, R.A., Evans, H.D., *Ind. Eng Chem. 43* (1951) No. 6, pp. 1317–1324.
[41] Slater, M.J., Unpublished work, 1989.
[42] Grace, J.R., Wairegi, T., Nguyen, T.H., *Trans. Inst. Chem. Eng 54* (1976) pp. 167–174.

Modelling of Pressure Drop in Packed Columns

Reinhard Billet and Michael Schultes*

The correct choice of packing is of decisive importance for optimum process efficiency in the operation of two-phase countercurrent columns. An important criterion for this choice is the pressure drop in the gas flow. Theoretical relationships are derived for calculating the pressure drop in beds with dry and trickle packings. It has been demonstrated by comprehensive experiments that these relationships allow the pressure drop to be determined more accurately than by previous methods. The experiments were performed at the Department of Thermal Separation Processes of Bochum University on 54 different packed beds, using 24 different systems.

1 Introduction

In the past few years, highly effective new packings have been developed for absorption, desorption and rectification columns, used for the separation of liquid and gas mixtures in the process industries. They feature minimum maldistribution, large interfacial areas and reduced pressure drops in the gas phase.

The differences between the geometry of the new types of packing and that of conventional designs necessitated a critical check of the existing design rules for calculating the pressure drop. Most equations found in the literature for its determination in absorption, desorption and rectification columns are empirical or semi-empirical. They have been derived largely from studies on conventional packings and cannot be unreservedly applied to modern designs. The aim of this paper is to develop a new theoretical model, valid for both conventional and modern types of packing, for the calculation of pressure drop in two-phase countercurrent columns.

* Prof. Dr.-Ing. R. Billet and Dr.-Ing. M. Schultes, Ruhr-Universität Bochum, Department of Thermal Separation Processes, D-4630 Bochum, Universitätsstraße 150.

In order to describe the flow in a packed trickle bed, it is assumed that the bed is equivalent to a multiplicity of flow channels through which the liquid of density[1)] ϱ_L and viscosity η_L flows downwards as a film of thickness s_o at a local velocity $\bar{u}_{L,S}$. If inertia forces are neglected, gravity and shear forces in the laminar-flow film, Eq. (1), are held in equilibrium with the frictional forces by the shear stress τ_V in the vapour at the surface of the film, Eq. (2). In Eq. (2), ϱ_V is the gas density, $\bar{u}_V$ the average effective gas velocity and ψ the resistance coefficient for gas flow [3]:

$$\frac{\mathrm{d}\left(\eta_L \frac{\mathrm{d}\bar{u}_{L,S}}{\mathrm{d}s}\right)}{\mathrm{d}s} = -\varrho_L\, g \quad , \tag{1}$$

$$\tau_V = -\psi \frac{\varrho_V\, \bar{u}_V^2}{2} \quad . \tag{2}$$

1) List of symbols at the end of the paper.

0930-7516/91/0204-0089 $03.50+.25/0

2 Pressure Drop in a Gas Stream Flowing through Dry Beds

The pressure drop $\Delta p_o/H$ of a stream of gas flowing through dry bed of height H can be determined from the shear force/pressure equilibrium and the Newtonian friction law. Eq. (3), in which d_h is the hydraulic diameter and ψ_o the resistance coefficient for the dry bed, can thus be derived from Eq. (2):

$$\frac{\Delta p_o}{H} = \psi_o \frac{4}{d_h} \frac{\varrho_V \bar{u}_V^2}{2} \quad . \tag{3}$$

The average effective gas velocity can be calculated as the ratio of the average gas velocity per unit cross-sectional area of column u_V to the void fraction ε, Eq. (4). The product of gas velocity and the square root of gas density yields the gas capacity factor F_V, Eq. (5). The hydraulic diameter d_h is fixed by the free bed volume $(V_S - V_P)$, where V_S is the column volume, V_P the bed volume and A_P the total area of packing. It can thus be described by the void fraction ε and the geometric area a per unit volume of packing, Eq. (6)

$$\bar{u}_V = \frac{u_V}{\varepsilon} \quad , \tag{4}$$

$$F_V = u_V \, \varrho_V^{1/2} \quad , \tag{5}$$

$$d_h = 4 \frac{V_S - V_P}{A_P} = 4 \frac{\varepsilon}{a} \quad . \tag{6}$$

Inserting Eqs (4)–(6) into Eq. (3) yields the following expression for the pressure drop per unit height, Eq. (7)

$$\frac{\Delta p_o}{H} = \psi_o \frac{a}{\varepsilon^3} \frac{F_v^2}{2} \quad . \tag{7}$$

In a real packed bed, the local void fraction differs from the theoretical value ε, depending on the column diameter d_S because there is more free space at the wall of the column. The difference can be accounted for by a wall factor K, Eq. (8). This gives Eq. (9) [6]

$$\frac{1}{K} = 1 + \frac{2}{3} \frac{1}{1-\varepsilon} \frac{d_P}{d_S} \quad , \tag{8}$$

$$\frac{\Delta p_o}{H} = \Psi_o \frac{a}{\varepsilon^3} \frac{F_v^2}{2} \frac{1}{K} \quad . \tag{9}$$

The resistance coefficient ψ_o in Eq. (9) must be determined empirically. Thus, Eq. (10) is based on the data obtained in experimental studies on 54 different types of packings. It includes the effect exerted on the gas flow by the vapour Reynolds number Re_V, defined by Eq. (11), in which ν_V is the kinematic viscosity of the gas and d_P the particle diameter. It is seen from Eq. (12) that the particle diameter depends on the ratio of the volume of packing V_P to its total area A_P and can thus be described by ε and a.

$$\psi_o = C_P \left(\frac{64}{\mathrm{Re}_V} + \frac{1.8}{\mathrm{Re}_V^{0.08}} \right) \quad , \tag{10}$$

$$\mathrm{Re}_V = \frac{u_V \, d_P}{(1-\varepsilon)\, \nu_V} K \quad , \tag{11}$$

$$d_P = 6 \frac{V_P}{A_P} = 6 \frac{1-\varepsilon}{a} \quad . \tag{12}$$

The term ψ_o defined by Eq. (10) is known from literature and has been confirmed by the studies carried out at the Department of Thermal Separation Processes of Bochum University. The constant C_P characterizes the geometry and surface properties of dry packing and is therefore specific for a given type of packing. Its values are listed in Tables 1a and 1b.

An example is presented in Fig. 1 which shows the pressure drop per unit height $\Delta p_o/H$ of a dry bed of 32 mm plastic Envipac rings as a function of the gas capacity factor F_V. The associated relationship between the resistance coefficient ψ_o and the gas Reynolds number Re_V is shown in Fig. 2. At low loads, the downward slope of the curve shown in Fig. 2 becomes steeper. In this range, up to Reynolds numbers of $\mathrm{Re}_V \approx 2100$, the gas flow is laminar, and the first summand in Eq. (10) governs the shape of the curve. Above this value, the flow becomes turbulent, and the second summand in Eq. (10) becomes the most decisive.

3 Pressure Drop in Gas Flows through Packed Trickle Beds

If the packing is wetted by a liquid, the column volume available for gas flow becomes reduced by the volume of the liquid fraction. Hence, if the volume of liquid in the bed V_L is expressed as a fraction of the column volume V_S, the liquid holdup h_L can be described by Eq. (13), and the effective void fraction ε_e by Eq. (14).

$$h_L = \frac{V_L}{V_S} \tag{13}$$

$$\varepsilon_e = (\varepsilon - h_L) \tag{14}$$

Eq. (15) is then obtained by substituting $\varepsilon_e = \varepsilon - h_L$ for ε in Eq. (9) and by introducing a wetting factor f_w which reflects the change in the packing surface area as a result of wetting. It is thus valid for determining the pressure drop per unit height in a packed trickle bed with a resistance coefficient for two-phase flow ψ_L:

$$\frac{\Delta p}{H} = \psi_L \frac{f_w \, a}{(\varepsilon - h_L)^3} \frac{F_v^2}{2} \frac{1}{K} \quad . \tag{15}$$

The excess pressure drop of the gas stream in the trickle bed over that in the dry bed corresponds to their ratio $\Delta p/\Delta p_o$, as expressed by Eq. (16)

$$\frac{\Delta p}{\Delta p_o} = \frac{\psi_L}{\psi_o} f_w \left(\frac{\varepsilon}{\varepsilon - h_L} \right)^3 \quad , \tag{16}$$

$$f(h_L) = \left(\frac{\varepsilon}{\varepsilon - h_L} \right)^3 \quad . \tag{17}$$

Table 1a. Characteristic data and constants C_P of Eqs (10) and (21) for dumped packings.

Dumped packings	Material	Size	N [$1/m^3$]	a [m^2/m^3]	ε [m^3/m^3]	C_P
Pall rings	Metal	50 mm	6242	112.6	0.951	0.763
		38 mm	15772	149.6	0.952	1.003
		35 mm	19517	139.4	0.965	0.967
		25 mm	53900	223.5	0.954	0.957
		15 mm	229225	368.4	0.933	0.990
	Plastic	50 mm	6765	111.1	0.919	0.698
		35 mm	17000	151.1	0.906	0.927
		25 mm	52300	225.0	0.887	0.865
	Ceramic	50 mm	6215	116.5	0.783	0.662
Ralu rings	Plastic	50 mm	5770	95.2	0.938	0.468
		50 mm,hydr.	5720	94.3	0.939	0.439
Hiflow rings	Metal	50 mm	5000	92.3	0.977	0.421
		25 mm	40790	202.9	0.962	0.689
	Plastic	90 mm	1340	69.7	0.968	0.276
		50 mm	6815	117.1	0.925	0.327
		50 mm,hydr.	6890	118.4	0.925	0.311
		25 mm	46100	194.5	0.918	0.741
	Ceramic	75 mm	1904	54.1	0.868	0.435
		50 mm	5120	89.7	0.809	0.538
		35 mm	16840	108.3	0.833	0.621
		20 mm,4 webs	121314	286.2	0.758	0.628
Hiflow rings Super	Plastic	50 mm	6050	82.0	0.942	0.414
NOR PAC rings	Plastic	50 mm	7330	86.8	0.947	0.350
		35 mm	17450	141.8	0.944	0.371
		25 mm,type B	47837	193.5	0.921	0.397
		25 mm,10 webs	44346	179.4	0.927	0.383
		22 mm	69274	249.0	0.913	0.397
		15 mm	193738	311.4	0.918	0.365
Raflux rings	Plastic	15 mm	193522	307.9	0.894	0.595
VSP rings	Metal	50 mm,no. 2	7841	104.6	0.980	0.773
		25 mm,no. 1	33434	199.6	0.975	0.782
Envipac rings	Plastic	80 mm,no. 3	2000	60.0	0.955	0.358
		60 mm,no. 2	6800	98.4	0.961	0.338
		32 mm,no. 1	53000	138.9	0.936	0.549
Top-pak	Aluminium	50 mm	6947	106.6	0.956	0.604
Bialecki rings	Metal	50 mm	6278	121.0	0.966	0.719
		35 mm	19303	164.4	0.965	1.011
		25 mm	55000	238.0	0.940	0.891
Raschig rings	Ceramic	25 mm	48175	185.4	0.662	1.329
Intalox saddles	Plastic	50 mm	8656	122.1	0.908	0.758
	Ceramic	50 mm	8882	114.6	0.761	0.747
Hiflow saddles	Plastic	50 mm	9939	86.4	0.938	0.454
Tellerettes	Plastic	25 mm	35365	182.0	0.900	0.538
Hackettes	Plastic	45 mm	12252	133.4	0.931	0.399

hydr. = hydrophilized.

Table 1b. Characteristic data and constants C_P of Eqs (10) and (21) for regular packings.

Regular packings	Material	Size	N [1/m³]	a [m²/m³]	ε [m³/m³]	C_P
Pall rings	Ceramic	50 mm	7502	155.2	0.754	0.233
Hiflow rings	Plastic	50 mm	7640	131.3	0.916	0.172
		50 mm,hydr.	8150	140.1	0.911	0.172
Ralu pak	Metal	YC-250		250.0	0.945	0.191
Impulse packing	Ceramic	100		96.7	0.828	0.417
Montzpak	Metal	B1-200		200.0	0.979	0.355
		B1-300		300.0	0.930	0.295
	Plastic	C1-200		200.0	0.954	0.453
		C2-200		200.0	0.900	0.481
Euroform	Plastic	PN-110		110.0	0.936	0.250

hydr. = hydrophilized

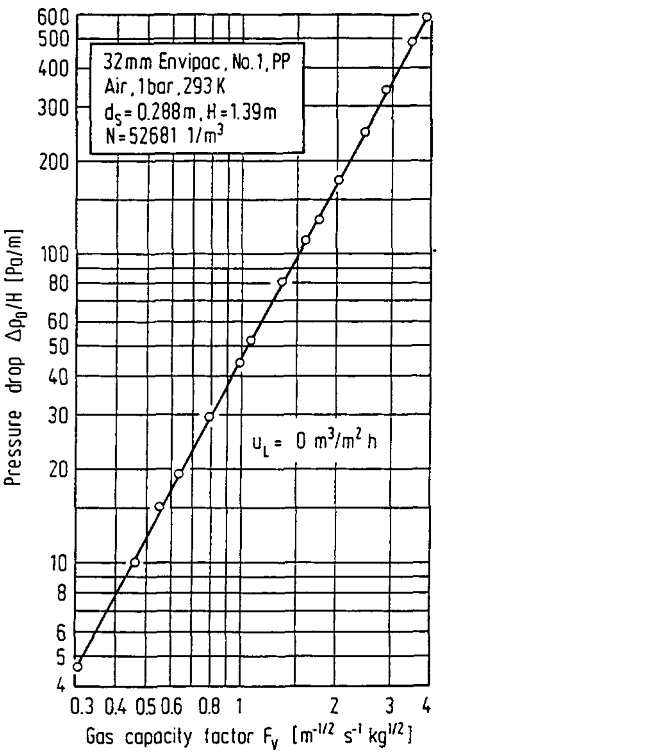

Fig. 1. Pressure drop of dry bed filled with 32 mm plastic Envipac rings as a function of gas capacity factor.

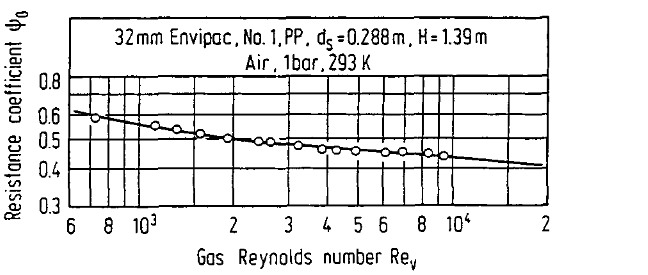

Fig. 2. Log-log plot of resistance factor for dry bed, packed with 32 mm plastic Envipac rings as a function of gas Reynolds number.

Eq. (16) indicates clearly that the increase in pressure drop can be described by the product of the ratio of resistance coefficients for two-phase and one-phase flow, the wetting factor f_w and an additional function $f(h_L)$, Eq. (17), in which the liquid hold-up is a quantity which depends on the load.

Solution of Eqs (1) and (2) leads to Eq. (18), which describes the liquid hold-up over the entire loading range up to the flood point; and to Eq. (19), which describes the liquid hold-up to the loading point [3–5,9]:

$$h_L = \left[\frac{a^2\,\eta_L\,u_L}{\frac{1}{3}\,g\,\varrho_L - \frac{1}{4}\,\psi_L\,\frac{a}{h_L(\varepsilon-h_L)^2}\,u_V^2\,\varrho_V}\right]^{1/3}, \qquad (18)$$

$$h_L = h_{L,S} = \left(\frac{12\,\eta_L\,u_L\,a^2}{g\,\varrho_L}\right)^{1/3}. \qquad (19)$$

Eq. (19) allows Eq. (17) to be solved and $f(h_L)$ shown graphically as a function of the liquid load u_L. This is demonstrated in Fig. 3, for which the 50 mm plastic Hiflow rings were taken as an example. As u_L decreases, the function $f(h_L)$ approaches a limiting value of unity because the liquid hold-up tends to zero and thus its effect subsides. The higher the value selected for the liquid load, the greater is the effect exerted by the liquid in the column on the value of the function $f(h_L)$ and the pressure drop will increase continuously.

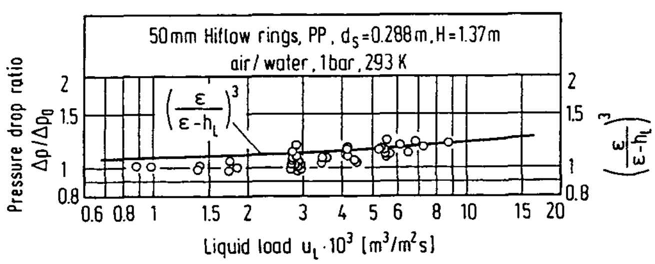

Fig. 3. Experimental pressure drop ratios and values of hold-up function versus liquid load for 50 mm plastic Hiflow rings.

Fig. 3 also shows the experimentally determined pressure drop ratios $\Delta p/\Delta p_o$ as a function of the liquid load. It can be seen that the function $f(h_L)$ reproduces the experimental values fairly accurately. Hence, a new equation (Eq. (20)) can be written for the pressure drop ratio $\Delta p/\Delta p_o$. As the liquid trickles through the bed, static hold-up occurs at the points of contact between the individual packings and in the interspaces, with the liquid forming a film on the surface of the packing. Hence, the surface structure differs from that during gas flow through a dry bed and this is reflected by the additional term $f(S)$ in Eq. (20):

$$\frac{\Delta p}{\Delta p_o} = f(S)\left(\frac{\varepsilon}{\varepsilon - h_L}\right)^x \quad . \tag{20}$$

Combining Eqs (16) and (20) and substituting the right hand side of Eq. (10) for ψ_o gives rise to Eq. (21) for the resistance coefficient ψ'_L for two-phase flow:

$$\psi'_L = \psi_L\, f_W = C_P\, f(S)\left(\frac{64}{Re_V} + \frac{1.8}{Re_V^{0.08}}\right)\left(\frac{\varepsilon - h_L}{\varepsilon}\right)^{(3-x)} \quad . \tag{21}$$

Eqs (15) and (21) were verified against the results obtained on a large number of packings. The verification included the effects exerted by the various physical properties of 24 different systems (see Table 2), including those intended for purely hydraulic studies and mixtures intended for absorption, desorption and rectification [1, 2]. Evaluation of thus obtained comprehensive data revealed that, in Eqs (20) and (21), the numerical value of exponent x was 1.5 and that the expression $f(S)$ could be replaced by a function Eq. (22), which depends on the Reynolds number of liquid Re_L, Eq. (23). Values of the constant C_P in Eq. (21) are listed together with the characteristic data of the various types of packing in Tables 1a and 1b.

$$f(S) = \exp\left(\frac{Re_L}{200}\right) \qquad \text{for } x = 1.5 \quad , \tag{22}$$

$$Re_L = \frac{u_L\, \varrho_L}{a\, \eta_L} \quad . \tag{23}$$

Empirical values of the pressure drop $\Delta p/H$ in a trickle bed of 32 mm plastic Envipac rings are plotted against the gas capacity factor F_V in Fig. 4. Fig. 5 shows the corresponding values of the resistance coefficient $\psi'_L = \psi_L f_W$ as a function of the liquid load u_L.

Mathematical prediction of the liquid hold-up h_L from Eq. (19) is restricted to the range extending up to the loading point. Fig. 6 shows the fundamental relationship between the liquid hold-up h_L and the ratio of gas velocity u_V to that at the flood point $u_{V,Fl}$. Up to the loading point S, h_L is practically independent of gas velocity and is equal to $h_{L,S}$. Above this point, the shear forces, acting in the gas, support the liquid film until the liquid hold-up at the flood point attains the value of $h_{L,Fl}$. These boundary conditions are described by Eqs (24) and (25).

1. Boundary condition: for $\frac{u_V}{u_{V,Fl}} = 0 \Rightarrow h_L = h_{L,S}$. (24)

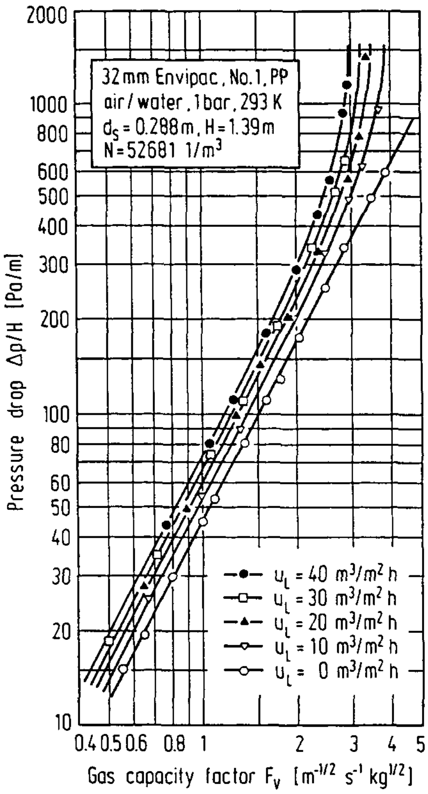

Fig. 4. Pressure drop of trickle bed with 32 mm plastic Envipac rings as a function of gas capacity factor at various liquid loads.

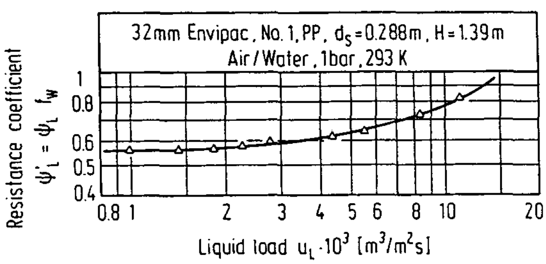

Fig. 5. Resistance factor for trickle 32 mm plastic Envipac rings as a function of liquid load.

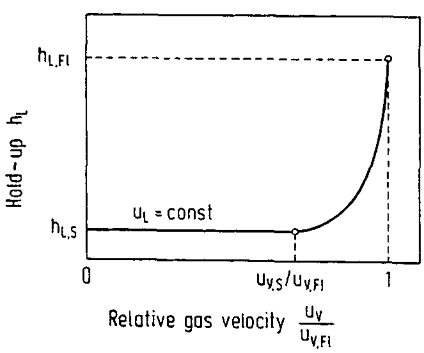

Fig. 6. Fundamental relationship between liquid hold-up and gas velocity for countercurrent flow columns.

2. Boundary condition: for $\dfrac{u_V}{u_{V,Fl}} = 1 \Rightarrow h_L = h_{L,Fl}$. (25)

Eq. (26) is an empirical equation which describes h_L in Fig. 6 and satisfies the boundary conditions

$$h_L = b + c \left(\frac{u_V}{u_{V,Fl}}\right)^n \quad . \tag{26}$$

Eq. (27) is then derived from Eqs (24) and (25), with an exponent $n = 13$, obtained from experimental investigations; $h_{L,S}$ in this equation is the hold-up as defined by Eq. (19) and $h_{L,Fl}$ is the liquid hold-up at the flood point, as given by Eq. (28) [3]. The term in parentheses in Eq. (28) accounts for the effect of viscosity and density of the substance (subscript L) compared to the corresponding values for water at 20 °C (subscript W).

$$h_L = h_{L,S} + (h_{L,Fl} - h_{L,S}) \left(\frac{u_V}{u_{V,Fl}}\right)^{13} \quad , \tag{27}$$

$$h_{L,Fl} = 0.3741\ \varepsilon \left(\frac{\eta_L\ \varrho_W}{\eta_W\ \varrho_L}\right)^{0.05} \quad \text{for } 0 < u_L < 200\ [\mathrm{m^3/m^2h}] \text{ and } \eta_L > 10^{-4}\ [\mathrm{kg/ms}] \quad . \tag{28}$$

Above the loading point, Eq. (22) must be modified by an empirical ratio which describes the excess liquid hold-up above this limit up to $h_{L,Fl}$; it becomes unity for the range below the loading point (cf. Eq. (29)).

$$f(S) = \left(\frac{h_L}{h_{L,S}}\right)^{0.3} \exp\left(\frac{Re_L}{200}\right) \quad . \tag{29}$$

A comparison of the pressure drops calculated from Eqs (9) and (10) for dry packed bed and from Eqs (15), (19), (21) and (22) for a packed trickle bed with the constant C_P of Tables 1a and 1b and the values, determined by experiments up to the loading point, reveals that the mean relative deviation is 9.1% (see Fig. 7).

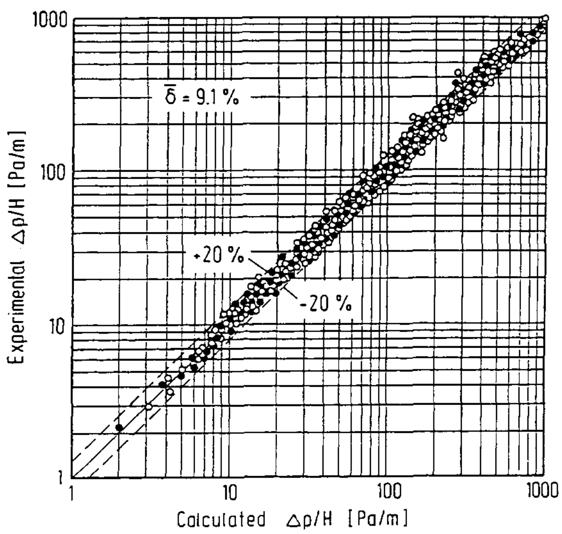

Fig. 7. Comparison of pressure drops of dry and trickle beds calculated from Eqs (9) and (15) with experimentally determined values.

Non-steady gas and liquid flow above the loading point makes the precise determination of pressure drop by experiment very difficult. Thus, the scatter range of measured values obtained from these studies is correspondingly larger.

The largest difference occurs in the vicinity of the flood point. Were the review to be extended to include a comparison between the values determined from Eq. (15) and the empirically determined pressure drops up to 90% of the flood point and if Eq. (27) were adopted for determining the liquid hold-up, the mean relative error would increase to 10.8%.

At very high liquid loads, the film becomes so thick that it coalesces in the narrow parts of the bed. As a result, extensive zones of the fractional free cross-section become filled, and a continuous layer of liquid is thus formed, through which the gas phase rises in the form of bubbles.

If this limiting load, which is referred to as the phase inversion point, is exceeded, the liquid hold-up and the resistance coefficient or the pressure drop in the gas flow increase at a disproportionately high rate. This phenomenon was first described by Elgin and Weiss and by Zenz [7, 8]. It occurs when certain flow parameters reach the value given by Eq. (30). At higher values, Eq. (15) no longer applies.

$$\frac{L}{V}\left[\frac{\varrho_V}{\varrho_L}\right]^{1/2} = 0.4 \quad . \tag{30}$$

4 Conclusions

The equations presented in this paper permit the pressure drop in the gas stream to be predicted mathematically up to the flood point in packed absorption, desorption and rectification columns. They are based on a theoretical model which accounts for the effects of physical, operational and design parameters on the flow of gas and liquid. For the determination of pressure drop, the knowledge of only one constant, specific for the packing, is required, regardless of whether the bed is trickle or dry.

The validity of the derived equations has been confirmed by the fact that the calculated values differ only slightly from the measured ones. The investigated parameters are compiled in Tables 2 and 3.

Received: December 22, 1989 [CET 272]

Symbols used

a	$[\mathrm{m^2/m^3}]$	total surface area per unit packed volume
A_P	$[\mathrm{m^2}]$	total surface area of packing
b		constant
c		constant
C_P		constant
d_h	[m]	hydraulic diameter
d_P	[m]	particle diameter
d_S	[m]	column diameter
f_w		wetting factor

Table 2. Pressure and physical properties of investigated systems.

Systems	p [mbar]	ϱ_V [kg/m³]	$\nu_V \cdot 10^6$ [m²/s]	ϱ_L [kg/m³]	$\nu_L \cdot 10^6$ [m²/s]
Air/water	1000	1.19	15.1	999	1.03
Air/methanol	1000	1.16	15.6	791	0.72
Air/turbine oil	1000	1.13	16.1	870	50.06
Air/machine oil 1	1000	1.15	15.8	885	58.76
Air/machine oil 2	1000	1.12	15.2	890	99.03
Air/ethylene glycol	1000	1.17	15.4	1115	16.14
NH_3-air/water	1000	1.18	15.1	999	1.03
NH_3-air/4% H_2SO_4 in H_2O	1000	1.18	15.2	1033	1.05
SO_2-air/1.78mol.NaOH in H_2O	1000	1.19	15.1	1039	1.15
CO_2-air/water	1000	1.19	15.1	1000	1.00
Methanol/ethanol	1000	1.30	8.5	738	0.52
Ethanol/water	1000	1.29	8.4	791	0.50
Chlorobenzene/ethyl benzene	33	0.14	46.0	963	0.60
Chlorobenzene/ethyl benzene	67	0.27	28.9	949	0.52
Chlorobenzene/ethyl benzene	133	0.51	15.9	926	0.45
Chlorobenzene/ethyl benzene	266	0.96	8.8	905	0.39
Chlorobenzene/ethyl benzene	532	1.80	4.9	886	0.34
Chlorobenzene/ethyl benzene	1000	3.28	2.9	866	0.30
Toluene/*n*-octane	100	0.35	20.8	839	0.52
Toluene/*n*-octane	133	0.46	16.4	833	0.49
Toluene/*n*-octane	266	0.90	8.5	763	0.43
Trans-decalin/*cis*-decalin	13	0.06	105.8	844	1.24
1,2-Dichloroethane/toluene	1000	3.22	2.9	924	0.38
Ethyl benzene/styrene	133	0.48	15.9	833	0.45

Table 3. Capacity range and test facilities.

Gas capacity factor	F_V	[m$^{-1/2}$ s^{-1} kg$^{1/2}$]	0.21 – 5.09
Liquid load	$u_L \cdot 10^3$	[m³/m²s]	0.17 – 16.7
Column diameter	d_s	[m]	0.15 – 0.80
Packed height	H	[m]	0.76 – 3.95
Interfacial area	a	[m²/m³]	54 – 380
Void fraction	ε	[m³/m³]	0.66 – 0.98
Number of investigated packings			54
Number of measurements			3296

F_V	[m$^{-1/2}$ s^{-1} kg$^{1/2}$]	vapour- or gas capacity factor
g	[m/s²]	gravitational acceleration
h_L	[m³/m³]	liquid hold-up
H	[m]	height
K		wall factor
L	[kg/s]	liquid mass flow rate
N	[1/m³]	packing density
n		exponent
Δp	[Pa]	pressure drop of trickle packing
Δp_o	[Pa]	pressure drop of dry packing
s	[m]	film thickness
$\bar{u}_L$	[m³/(m² s)]	liquid load
$\bar{u}_L$	[m/s]	average effective liquid load
u_V	[m³/(m² s)]	superficial vapour- or gas velocity
$\bar{u}_V$	[m/s]	mean effective vapour- or gas velocity
V	[kg/s]	mass flow rate of gas or vapour
V_L	[m³]	liquid volume
V_P	[m³]	volume of packing
V_S	[m³]	volume of column

Greek symbols

ε	[m³/m³]	void fraction
ε_e	[m³/m³]	effective void fraction
η	[kg/(m s)]	viscosity
ν	[m²/s]	kinematic viscosity
ϱ	[kg/m³]	density
ψ_L, ψ_L'		resistance coefficient of trickle packing
ψ_o		resistance coefficient of dry packing
τ_v		shear stress

Subscripts

Fl	flood point
L	liquid
o	surface
S	loading conditions
V	vapour or gas
W	water

Dimensionless numbers

$$Re_L = \frac{u_L \, \varrho_L}{a \, \eta_L}$$ Reynolds number of liquid

$$Re_v = \frac{u_V \, d_P}{(1-\varepsilon) \, \nu_V} K$$ Reynolds number of gas or vapour

References

[1] Billet, R., *Industrielle Destillation*, Verlag Chemie, Weinheim 1973.

[2] Billet, R., *Distillation Engineering*, Chemical Publishing Company, New York 1979.

[3] Billet, R., *I. Chem. Symp. Ser.* (1987) No. 104, pp. A171–A182.

[4] Billet, R., Schultes, M., *I. Chem. Symp. Ser.* (1987) No. 104, pp. A159–A170.

[5] Billet, R., Schultes, M., *I. Chem. Symp. Ser.* (1987) No. 104, pp. B255–B266.

[6] Brauer, H., *Grundlagen der Einphasen- und Mehrphasenströmung*, Sauerländer Verlag, Aurau 1971.

[7] Elgin, J.C., Weiss, F.B., *Ind. Eng Chem. 31* (1939) pp. 435–445.

[8] Zenz, F.A., *Chem. Eng Prog. 8* (1947) pp. 415–428.

[9] Billet, R., *Chem. Eng. Technol. 11* (1988) No. 3, pp. 139–148.